

Intelligent Image Restoration Approach: Using Neural Networks to Eradicate Dilemma in Punctual Kriging

Asmatullah Chaudhry^{1,2}, Asifullah Khan³, and Jin Young Kim¹, Quan Qi Niu¹

¹School of Electronics & Computer Engineering, CNU, Gwangju, South Korea

²HRD, PINSTECH, P.O. Nilore, Islamabad, Pakistan

³Department of Computer & Information Sciences, PIEAS, Nilore, Islamabad, Pakistan

asmat@jnu.ac.kr, asif@pieas.edu.pk, beyondi@jnu.ac.kr, newpoe@qq.com

Abstract: We report an intelligent image restoration approach by combining the geostatistical interpolation technique of punctual kriging and the machine learning approach of adaptive learning. Digital images degraded from Gaussian white noise are restored by first utilizing fuzzy logic for selecting pixels that need to be kriged. The concept of punctual kriging is then used to estimate the intensity of a pixel. Kriging un-biased estimates mostly suffer from occurrence of negative weights and matrix inversion failure problems. Approximation is usually used to avoid these problems in punctual kriging based image restoration. Artificial neural networks (ANN) are employed to minimize the cost function of the kriging based pixel intensity estimation procedure. ANN, in merit to analytical methodologies, avoids both matrix inversion failure and negative weights problems. Experimental results using four hundred and fifty images and different image qualitative measures show the superiority of the proposed method against adaptive Weiner filter and existing fuzzy kriging approaches. This also validates the use of hybrid approaches to image restoration problem.

[Chaudhry A, Khan A, Kim JY, Niu QQ. **Intelligent Image Restoration Approach: Using Neural Networks to Eradicate Dilemma in Punctual Kriging.** *Life Sci J* 2013;10(1):1631-1641] (ISSN: 1097-8135). <http://www.lifesciencesite.com>. 240

Keywords: Image restoration, Artificial neural networks (ANN), Punctual kriging, Matrix inversion failure, Negative Weights.

1. Introduction

Image restoration is a branch of image processing that helps restore an image after it has been degraded. One of the primary tasks in developing image restoration techniques is noise removal without destroying edge information. Noise smoothing and edge enhancement are generally considered as conflicting tasks. Since smoothing a region might destroy an edge while sharpening edges might lead to amplification of unnecessary noise (Voloshynovskiy et al., 2005), therefore, we present a new spatial filtering technique; a neural approach based on punctual kriging and fuzzy logic control, to consider this conflict and to remove noise while efficiently preserving the image details and edge information.

Punctual kriging, named after its developer, *D. G. Krige* (1951) is heavily used in mining and geostatistics based applications. It is an interpolation technique that gives an optimal linear estimate of an unknown parameter at a sampling point in terms of its known values at the surrounding sampling points (Wackernagel and Geostatistics, 2003). The estimation involves calculation of the semi-variances and modeling of semi-variograms from the sampled data. Besides this, kriging has been applied in many other fields as well.

Fuzzy filters have been extensively applied in image processing over the last decade. *Choi* and

Krishnapuram (1997) devised fuzzy rule based multiple filters, derived from the method of weighted least squares, for noise removal. Some researchers have also investigated the use of fuzzy clustering for the removal of impulsive noise (Doroodchi and Reza, 1996). In (Farbiz and Menhaj, 2000), authors have introduced an approach of image filtering based on fuzzy logic control. They have shown how to remove impulsive noise and smooth out Gaussian noise while, simultaneously, preserving image details and edges efficiently. *Liang and Looney* (2003) have proposed a competition fuzzy edge detector to distinguish the noisy pixels from the edge pixels. Further, *Khriji and Gabbouj* (2004) have recently proposed a fuzzy transformation based approach for multichannel image processing. Although fuzzy spatial filters have been widely used, however, with the increase of local information, the number of fuzzy rules also increases accordingly. To reduce the requirement of such complicated rules, fuzzy control is used as a complementary tool along with the existing techniques to develop better and accurate methods. This is one of the major aims of the investigations presented in this paper.

In the most basic image restoration approach using neural networks, noise is removed from the image by simple filtering. Cellular neural networks by *Chua and Yang* (1988) have been proposed for noise suppression. Improvements have been done for

training cellular neural networks that make use of genetic algorithms by *Zamperelli* (1997). Generalized adaptive neural filter (Hanek and Ansari, 1996), (Zhang and Ansari, 1996) is another interesting neural architecture for noise filtering. It consists of a set of neural operators based on stack filters (Ansari and Zhang, 1993) that make use of binary decomposition of gray valued data.

Combination of order statistic filters and Hopfield neural network have also been developed and used by *Qian et al.* (1993) for noise removal and image de-blurring. *Suetake and Uchino* (2007) have proposed a radial basis function network and Wiener hybrid filter to exploit merits of both for removing noise with an arbitrary distribution. Multilevel sigmoidal activation functions (Sivakumar and Desai, 1992) are used by *Sivakumar et al.* to model a blurred and noisy image with many gray levels without any knowledge of the statistics of the additive noise and blurring function. *Widyanto et al.* (2005) have proposed a method to improve recognition as well as generalization capability of back-propagation neural network as a hidden layer self-organization inspired by immune algorithm. Recently, *Alex et al.* (2002) have introduced a spatially regularized neural approach that makes use of local image statistics to apply varying regularization to different areas of the image by using a parallel implementation of the Hopfield neural network.

Pham and Wagner (2000), (1999) have used punctual kriging along with fuzzy sets to enhance images corrupted by Gaussian white noise. They model soft-thresholding by fuzzy sets. In their approach, the pixel intensity in the processed image is a weighted sum of the original (noisy) and the estimated value through kriging. They have evaluated their results qualitatively in comparison with adaptive Wiener filter. However, their study does not provide any quantitative performance analysis of their proposed technique (Mirza and Munir, 2004), (Asmatullah, 2007). In addition, they apply kriging to all pixels in the degraded image. Considering 3×3 neighborhood, inverse of a kriging matrix of size 9×9 is required, that can make the filtering process computationally expensive. In addition, due to a zero diagonal, inverse of the kriging matrix may not always be possible. The filter weights also suffer from the problem of negative values, and an approximation is used to estimate the pixel under consideration by renormalizing the positive weights which leads to an overall poor performance of the filter. This paper is an extension of our previous work (Asmatullah, 2007), (Mirza et al., 2007) and aims at improving upon the existing fuzzy-kriging approach and to avoid various constraints in punctual kriging based image restoration by introducing a new hybrid

technique based on fuzzy inference system, neural net and punctual kriging. This paper makes the following contributions:

1. Introduce an effective hybrid neuro-fuzzy based kriging methodology for image denoising.
2. Solve both the problems of matrix inversion failure and the negative weights in punctual kriging by exploiting learning capabilities of artificial neural network (ANN).

For clarity and understanding, first we present in Table 1:

Table 1. The abbreviations used in the text.

<i>FIS</i>	Fuzzy Inference System
<i>MSE</i>	Mean Squared Error
<i>PSNR</i>	Peak Signal-to-Noise Ratio
<i>wPSNR</i>	Weighted Peak Signal-to-Noise Ratio
<i>SSIM</i>	Structure Similarity Index Measure
<i>VMSE</i>	Variogram based Mean Squared Error
<i>VPSNR</i>	Variogram based Peak Signal-to-Noise Ratio
<i>BPN</i>	Back-Propagation Neural Network
<i>AWF</i>	Adaptive Wiener Filter
<i>PWFK</i>	Pham & Wagner Fuzzy Kriging
<i>SAFK</i>	Spatially-Adaptive Fuzzy Kriging

Rest of the paper is structured as follows. Section 2 introduces punctual kriging and variograms, fuzzy inference system and fuzzy averaging. It also presents some review of ANNs used for image restoration and few of the most commonly used image quality measures along with the proposed variogram based quality measure. Section 3 explains the proposed hybrid technique based on punctual kriging and the neuro-fuzzy approach of adaptive learning. Experimental results along with their discussion are presented in section 4. Our findings including directions for future work are given in section 5.

2. Theory

2.1. Punctual Kriging and Variograms

Punctual kriging provides the best linear unbiased estimate of an unknown point on a surface (El-Sheimy et al., 2005). The estimate is the weighted sum of the known neighboring values around the unknown point. The weights are determined to minimize the variance of the estimation-error. To achieve this, kriging uses a variogram model (a concept from geostatistics). Based on the variogram model chosen, known values are assigned optimal weights to calculate the unknown value. Variogram presents the variation of semivariance with respect to distance from a point. Semivariance provides a measure of spatial dependence between samples. Semivariance (Wackernagel and Geostatistics, 2003) of the samples at lag 'd' can be calculated from eqn. (1).

$$\gamma(d) = \frac{1}{2} \text{Var}(z_{i+d} - z_i) \tag{1}$$

Different distance metrics can be used to identify a group of neighboring samples having the same lag. In the present investigations, however, we have considered the Euclidean metric as the distance measure. The experimental semivariogram is obtained directly by using the sample values from the experimental data.

For a given lag ‘d’, it is calculated from the available data as:

$$\gamma(d) = \frac{1}{2N(d)} \sum_{i=1}^{N(d)} (z_i - z_{i+d})^2 \tag{2}$$

The above expression for experimental semivariogram depends upon the spatial configuration of the available image data. One has to consider different cases, as to whether the data is aligned or not and whether it is regularly spaced along the alignments. However in the present case of digital images, the data is aligned and regularly spaced, which makes the estimation of the semi-variogram easy.

Punctual kriging is a linear combination of the neighboring sample values, as given by eqn. (3).

$$\hat{z} = \sum_i w_i z_i \tag{3}$$

where, w_i are the weights and z_i are the neighboring values of z . It is an unbiased estimator if the weights add up to 1. This additional constraint on weights is given by:

$$\sum_i w_i = 1 \tag{4}$$

Statistical variance is measure of how different the estimated value is from its neighboring sample values. It can be found using the eqn. (5).

$$\text{Var}(e) = \text{Var}(z - \hat{z}) \tag{5}$$

A number of such linear unbiased estimators are available, but we find the *best* one in the sense that it has the smallest estimation variance. Thus, the cost function is defined as:

$$\phi(w_i, \lambda) = \text{Var}(e) - 2\lambda \left(\sum_i w_i - 1 \right) \tag{6}$$

where λ is the Lagrange multiplier. Differentiating the cost function $\phi(w_i, \lambda)$ with respect to w_i and λ , and setting the differential equal to zero and rearranging the system of equations, these can be written in matrix form as:

$$\begin{pmatrix} \gamma(d_{11}) & \gamma(d_{12}) & \dots & \gamma(d_{1n}) & 1 \\ \gamma(d_{21}) & \gamma(d_{22}) & \dots & \gamma(d_{2n}) & 1 \\ \vdots & \vdots & \ddots & \vdots & \vdots \\ \gamma(d_{n1}) & \gamma(d_{n2}) & \dots & \gamma(d_{nn}) & 1 \\ 1 & 1 & 1 & 1 & 0 \end{pmatrix} \begin{pmatrix} w_1 \\ w_2 \\ \vdots \\ w_n \\ \lambda \end{pmatrix} = \begin{pmatrix} \gamma(d_1) \\ \gamma(d_2) \\ \vdots \\ \gamma(d_n) \\ 1 \end{pmatrix} \tag{7}$$

or in matrix-vector notations

$$Aw = b \tag{8}$$

The A matrix is symmetric and has zero diagonal elements. The elements of the matrix are taken from the semivariogram (defined in eqn. (1)) for the current point. Solving eqn. (8) gives us the optimal kriging weights $\{w_1, w_2, \dots, w_n\}$ for estimating the unknown value \hat{z} using its neighbors. However, if A is a singular matrix, punctual kriging fails to estimate pixel intensity.

2.2. Fuzzy Inference System and Fuzzy Smoothing

There are two types of FIS, that are commonly used i.e. Mamdani and Takagi-Sugeno type (Driankov et al., 1993). Both types of FIS are similar in many aspects; fuzzifying the inputs and applying the fuzzy operator. The Takagi-Sugeno output membership functions are either linear or constant and this aspect mainly differs from the Mamdani type (Sugeno, 1985). In the proposed approach, the fuzzy output nonlinear membership functions are employed to decide the fate of a pixel. Therefore, we have used Mamdani type FIS because the decision making of whether a pixel needs to be estimated or not, depending upon the local properties of the neighborhood is a complex problem which could not be easily learned by linear membership functions (Mirza et al., 2007). Many researchers have proposed a variety of fuzzy logic based smoothing filters. These include fuzzy rank selection filter, fuzzy weighted filter, switching fuzzy filter and fuzzy neural network filter (Nachtegeal, 2000), (Liu and Li, 2004). However, we use a neuro-fuzzy filter in our approach.

In the present work, we have used both fuzzy based intelligent decision-making and fuzzy smoothing to improve the performance of the proposed spatial neuro-fuzzy filter. The main use of the fuzzy inference system is to generate a fuzzy map from the degraded image, which is then employed by the neuro-fuzzy filter to enhance the degraded image. Further, fuzzy smoothing is used to smooth out the unselected pixels within the proposed filter.

2.3. Artificial Neural Networks

The functional strength of ANN has already been demonstrated by many researchers in different areas such as pattern recognition and classification (Rudasi and Zahorian, 1991), (El Sherif and Abdel Samee, 1994), (Takahashi et al., 1994), (Khan et al., 2009), (Khan et al., 2008) image restoration (Greenhil and Davies, 1994), and machine vision (Jochem et al., 1995), (Pomerleau, 1992). Consequently, we use ANN to solve the set of

equations obtained in punctual kriging. Section 3 explains the mechanism of exploiting backpropagation training algorithm for this purpose and thus avoiding the problem of matrix inversion failure and negative weights.

2.4. Image Quality Measures

Besides MSE, PSNR, wPSNR and SSIM (Chaudhry et al, 2007), another image quality measure in terms of the experimental variograms of the original and degraded images is also used. Where by, if $\gamma_o(d)$ and $\gamma(d)$ represent the semi-variances at lag d of the original and degraded image respectively, then a variogram based image quality measure VMSE and VPSNR can be calculated as:

$$VMSE = \frac{1}{M_d} \sum_{d=0}^{M_d} [\gamma_o(d) - \gamma(d)]^2 \quad (9)$$

$$VPSNR = 10 \log_{10} \frac{[\max\{\gamma_o(d)\}]^2}{VMSE} \quad (10)$$

Here M_d is the maximum lag for the images.

VMSE and VPSNR are global quality measures; however, these do take into account the structural detail information present in the image. Variogram illustrate the variation of semivariance with respect to distance from a point, and semivariance provides a measure of spatial dependence between pixels. Variogram of two different images is different because both images have different distribution of data that can be verified from figure 4. Further, variogram of an image corrupted with white Gaussian noise shows the up-lifting of the variogram as the noise variance is increased. Furthermore, the general shape and structure of the variogram remains the same for low noise variances as shown in figure 5.

The hypothesis in developing this image quality measure relies on the idea that if a technique which brings the variogram of the restored image very close to that of the original image, will perform better. It can also be verified from Table 2 and figure 8. Statistical meaning of VMSE is to measure the mean squared error of the variogram of the estimated and the original images.

3. The Proposed Approach

The occurrence of singular matrix in kriging is inherently unpredictable as it depends on the variogram for a pixel in the degraded image. The variogram itself depends on neighboring values of a pixel. Such scenarios should be taken care of separately by replacing the processed pixel with a value given by fuzzy ‘averaging’ or ‘median’ filter, which ever makes the error variance ‘small’.

Table 2 shows the statistics about the number of pixels selected for kriging through fuzzy decider. It is observed that for about 88% of the selected pixels, the punctual kriging procedure results in negative weights. To handle this problem, approximation has been used to reinitialize the weights i.e. negative weights have been set to zero and positive weights have been renormalized. Also, for some pixels, the kriging procedure fails due to the problem of matrix inversion failure. It can be observed from the results shown in Table 2 that the actual number of pixels where punctual kriging is applied successfully (less than 12%) is far less than the pixels where it is unsuccessful (88%). This leads us to introduce some methodology in order to apply successful estimation of the selected pixel.

Table 2. Statistics of the pixels selected for kriging by the fuzzy decider. The Boat image degraded with white Gaussian noise of different variances.

Statistics of the data	White Gaussian Noise of different variance					
	0.1	0.08	0.06	0.04	0.02	0.01
No. of pixels advised for kriging	206215	190083	165535	124774	54927	13857
Matrix inversion failure	672	580	475	357	203	54
Parseval theorem violation	180767	168841	149946	116606	53329	13561

Fig. 1 shows the basic architecture of our proposed methodology. Firstly, we generate a map for pixels to be kriged or not through fuzzy decider. These selected pixels are estimated using neural network based punctual kriging. The pixels that are

not selected for kriging by the fuzzy decider are processed using the robust fuzzy weighted filter. Lastly, various image quality measures have been employed to analyze the quality of the processed image.

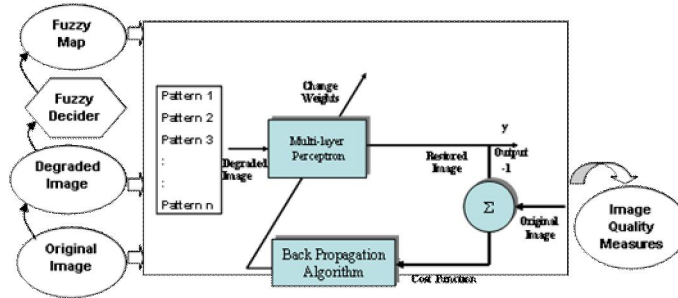


Figure 1. Schematic flowchart of the proposed neuro-fuzzy kriging filter

3.1. Details of Different Stages of the Proposed Methodology

In the proposed method, all pixels are not blindly kriged. Rather, based on the homogeneity and deviation of its local neighborhood, a pixel is selected for kriging by a fuzzy logic rule-based system. This fuzzy system is called the Fuzzy Decoder in our work. The inputs to the Fuzzy Decoder are a measure of homogeneity and DAMdistance which is based on the mean and deviation of the 3x3 window around the current pixel. The degree of homogeneity is estimated by eqn. (11) as proposed by Tizhoosh (2000). The numerator in eqn. (11) is the difference of the maximum and minimum gray values in the region comprising of the 3x3 window around a pixel, whereas, the denominator is the difference of the maximum and minimum gray values in the whole image.

$$\mu_H = \left(\frac{g_{max}^{local} - g_{min}^{local}}{g_{max}^{global} - g_{min}^{global}} \right) \quad (11)$$

The shapes of membership functions (as shown in Fig. 2 & 3) are set empirically to make a tradeoff between smoothness and edge preservation. The DAMdistance in the rules is simply the difference between the gray value of the current pixel and the mean gray value of its neighbors. The Fuzzy Decoder is a basic Mamdani-type fuzzy logic system consisting of the following rules.

If Homogeneity is High or DAMdistance is Low
then Do Not Perform Kriging
If Homogeneity is Low or DAMdistance is Very-High
then Perform Kriging

We have observed that spatial intensity variation is effectively represented with the two rules based on homogeneity and DAMdistance. The membership functions of homogeneity; Low and High, have been set as Gaussian (Fig. 3). The effectiveness of High membership function is dominant as compared to Low membership function in a small range of [0-0.1]. While, the effectiveness

of Low membership function is dominant in a relatively large range of [0.1-1]. Consequently, we make it sure that if the intensity of the pixel under consideration is close to that of the neighboring pixels (homogeneous region) then it is not a noisy pixel. Else, it is strictly considered as a noisy pixel and subsequently it is smoothed out. Similarly, the membership functions of DAMdistance; low and veryHigh, have been set as Gaussian (Fig. 2). In this case, low membership function is dominant in the range [0-87], while veryHigh remains dominant in the range [88-255]. This means that if the difference in intensity of the current pixel with that of the mean intensity of the rest of 8 pixels is small (less than 87 in this case), the probability of the current pixel being noisy is less and vice versa.

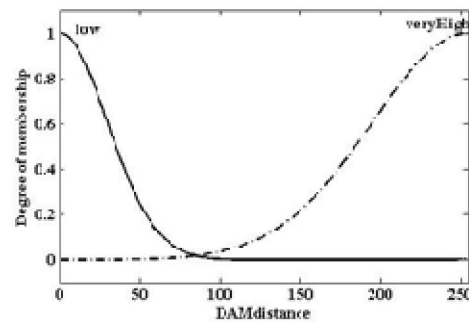


Figure 2. Membership function for DAMdistance

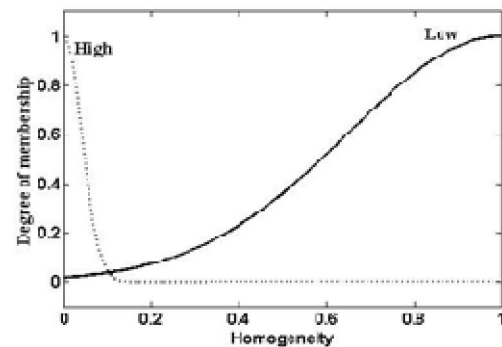


Figure 3. Membership function for Homogeneity

The proposed method has the following three stages.

3.1.1. Generation of Fuzzy Map

In the first stage, the noisy image is presented to the Fuzzy Decider that generates a binary image called the fuzzy decision map. This decision map is provided to the BPN based estimation stage, where the decision of whether to estimate or not estimate is enforced. This helps reduce the computational time quite effectively.

3.1.2. Employing BPN for Estimation

In the proposed approach, we have applied multilayer perceptron with back-propagation algorithm to estimate the pixels under consideration using the concept of punctual kriging. The BPN algorithm with modified cost function has been applied to train the neural net.

Architecture of the Network

The network configuration used for estimation of the pixels is given below.

Input Layer: Nine neurons
 Hidden Layer: Thirty five neurons
 Output Layer: One neuron
 Activation Function: Binary sigmoidal function.

$$f(x) = \left(\frac{1}{1 - \exp(-\beta x)} \right) \quad (12)$$

In our case, the slope parameter β is set equal to 1. Noisy image sub-pattern of size 3x3 is fed as input to the input layer of the neural network; neurons in the hidden layer are empirically set to 35. Binary sigmoidal function is used as an activation function to keep the output of the network within range 0 to 1 because this is the required pixel intensity range of the estimated image. And to train the neural network, 1000 epochs have been run. The initial conditions of the neural net have been set randomly to avoid its trapping in local minima.

Cost Function and Updating Weights

The standard backpropagation algorithm consists of two parts: forward-propagation and error backpropagation. We modify the error backpropagation part to minimize a new cost function. The error signal is the variance of the output of neural net and the target as given in eq. (5). The energy function or the Augmented Lagrangian is formed by incorporating the constraints and extra penalty terms. We modify the cost function by including the variance of estimation error, weights related constraint (the sum of weights should be equal to one) and extra penalty term.

$$L(w, v, \lambda, \kappa) = Var(e_n) + \lambda \left(\sum_{j=1}^m \sum_{k=1}^n w_{jk} - 1 \right) + \kappa \sum_{j=1}^m \sum_{k=1}^n w_{jk}^2 \quad (13)$$

Since there is only one neuron in the output layer, so we omit the subscript 'k' from eqn. (13)

$$L(w, v, \lambda, \kappa) = Var(e_n) + \lambda \left(\sum_{j=1}^m w_j - 1 \right) + \kappa \sum_{j=1}^m w_j^2 \quad (14)$$

where ' κ ' is the positive penalty factor.

Updating Weights in our Proposed Methodology

Case-I: For output layer

The correction in output layer weights Δw_j is proportional to the instantaneous gradient $\frac{\partial L}{\partial w_j}$. By differentiating eqn. (14) with respect to output layer

$$\frac{\partial L}{\partial w_j} = \frac{\partial Var(e_n)}{\partial w_j} + \lambda + 2\kappa \sum_{j=1}^m w_j \quad (15)$$

The correction term Δw_j applied to the output layer weights w_j is defined by

$$\Delta w_j = -\alpha \frac{\partial L}{\partial w_j} \quad (16)$$

where α is learning rate parameter, negative sign in eqn. (16) accounts for gradient decent in weight

space. Replacing the value of $\frac{\partial L}{\partial w_j}$ in eqn. (16),

$$\Delta w_j = -\alpha \left[\delta_y \cdot z_j + \lambda + 2\kappa \sum_{j=1}^m w_j \right] \quad (17)$$

Similarly, differentiating eqn. (14) with respect to λ , we obtain

$$\frac{\partial L}{\partial \lambda} = \sum_{j=1}^m w_j - 1 \quad (18)$$

Thus, weights and Lagrange multiplier updates will be

$$w_j(n+1) = w_j(n) + \Delta w_j(n)$$

$$\lambda(n+1) = \lambda(n) + \mu \left(\sum_{j=1}^m w_j(n) - 1 \right) \quad (19)$$

where, μ is learning rate parameter for Lagrange multiplier

Case-II: For hidden layer

Let us consider Neuron 'j' as a hidden node. In this case, we do not know what should be the desired response of the neuron, so we cannot calculate $Var(e)$ directly. However, from eqn. (13),

$$\frac{\partial L}{\partial v_{ij}} = \frac{\partial Var(e)}{\partial v_{ij}} \quad (20)$$

Thus, the correction term Δv_{ij} applied to the hidden layer weights is defined by

$$\Delta v_{ij} = -\alpha \cdot \frac{\partial L}{\partial v_{ij}} = -\alpha \frac{\partial Var(e)}{\partial v_{ij}} \quad (21)$$

Replacing the value of $\frac{\partial Var(e)}{\partial v_{ij}}$ in eqn. (21),

$$\Delta v_{ij} = -\alpha \left[\delta_y \cdot w_j \cdot f'(Z_{inj}) \cdot x_i \right] \quad (22)$$

Thus, hidden layer weights update will be

$$v_{ij}(n+1) = v_{ij}(n) + \Delta v_{ij}(n) \quad (23)$$

Training and Testing of the Net

In the second stage, three images of Cameraman, Lena and PCB are corrupted with white Gaussian noise of variance 0.1. The backpropagation neural network is trained through supervised learning on 3 x 3 image sub-patterns that constitute 10% of the flagged pixels of Cameraman, Lena and PCB images. However, these 10% 3x3 image sub-patterns are randomly picked from the degraded image, so that a general pattern of noise is learned by the BPN. To perform the image restoration simulation studies, we have used our Matlab based implementation of BPN. The developed BPN code is more general and enough to accept any number of neurons/layers (Tizhoosh, 2000), (Asmatullah et al., 2003). Simulation study has been carried out on IBM compatible Intel P-IV, 2.6 GHz machine. During the training phase, in each epoch, we shuffle the order in which these sub-patterns are being fed as an input to the network to avoid the network being trapped in the local minima. After training, the neural net has been tested against various images corrupted with white Gaussian noise of different variances.

3.1.3. Fuzzy Smoothing of Pixels Not Selected for Kriging

In the third stage, the unselected pixels by the Fuzzy Decider are processed using the robust fuzzy weighted filter. After the second stage, the processed image contains two types of values based on the decision map: kriging estimate through neural net and original values (unselected pixels). In this stage, a fuzzy smoothing is applied on the unselected pixels.

4. Results and Discussions

4.1. Variograms of the Original and Degraded Images

The experimental semi-variograms of three different types of images (Boat, Blood cells and Lena) have been computed and shown in Fig. 4. The shapes of the variograms for all three images near lag zero are continuous. This shows that the pixel values do not change abruptly at lags near zero. However, for Lena and Boat images, fluctuations start

appearing for lags greater than 10. This shows that after a lag of 10 pixels, we enter into a new region. Further, in case of Blood cells image, the fluctuations appear after a lag of 20 pixels. The variograms show sharp changes for larger lags.

Fig. 5 shows the changes in the experimental variogram when a zero mean Gaussian noise with various variances is added to a particular image. The most interesting aspect to note is the up-lifting of the variogram as the noise variance is increased (see Fig. 5(d)). It is also important to note that the general shape and structure of the variogram stays the same for low noise variances. The abrupt changes in the variogram take place at the same lags. Even for high noise variance, the shape of the variogram remains similar to that of the original image; however, the abrupt changes become more discontinuous. Further, near zero lag, the variogram becomes highly discontinuous as the additive noise variance is increased. These observations have led us to introduce the variogram based image quality measure VMSE, as introduced in section 4.

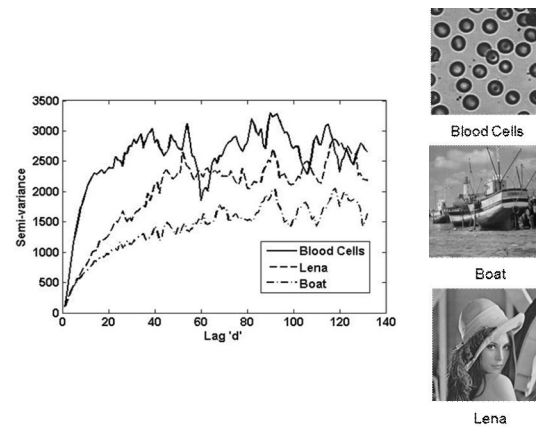


Figure 4. Experimental variograms of three different images

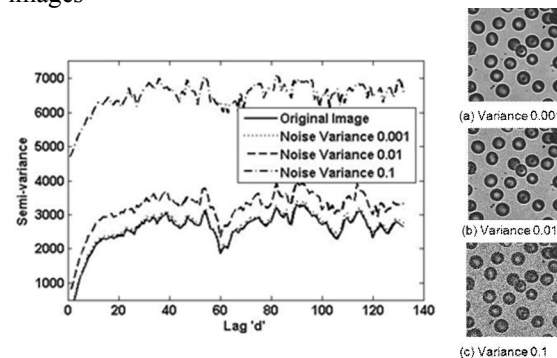


Figure 5. (a) – (c) Gaussian noise corrupted images with zero mean and different variances, (d) Variograms of Blood cells image with additive Gaussian white noise

Various image quality measures as explained in section 2 are applied to find out the quality of the processed image as compared to the original image. We have tested the performance of our approach by considering two scenarios.

Firstly, the performance of the proposed method has been tested for additive Gaussian white noise of different variances for a test image. Secondly, the performance is tested for different images corrupted with Gaussian white noise of same variance. This is because the effect of noise may change with the variance of noise as regards the visual distortion for the same image. On the other hand, same noise may affect different images differently as regards the visual distortion. Typical results from the Fuzzy Decider are shown in Fig. 6. The white pixels are the ones that need to be kriged.



Figure 6. Result from Fuzzy-Decider for Cameraman image degraded with variance 0.02

4.2. Scenario 1

In the first case, we have considered Boat image as a test image. The image is degraded with Gaussian white noise of variances ranging from 0.01 to 0.15. The results obtained from our approach have been compared with that of the AWF, PWFK, and SAFK approach. The effect of the additive Gaussian noise and its removal by various approaches are shown in Fig. 7. Table 3 gives a quantitative comparison between different methods in terms of MSE, PSNR, SSIM and VMSE. It can be observed that the proposed method offers superior performance against the white Gaussian noise of different variances as compared to rest of the methods.

The experimental variograms of the original, noisy, and restored images through AWF, PWFK, SAFK and proposed approach are plotted in Fig. 8. The image is corrupted with Gaussian noise of variance 0.08. From Fig. 8, it is clear that variograms of both the original as well as noisy image retain the structural information about the image and differ only in the semivariance at different lags depending upon the strength of the noise variance. Further, in comparison to the variograms produced by other methods, our approach produces a variogram that overlaps with the variogram of the original image. This is also clear from Table 3, where the VMSE is minimum compared to the other image restoration techniques.

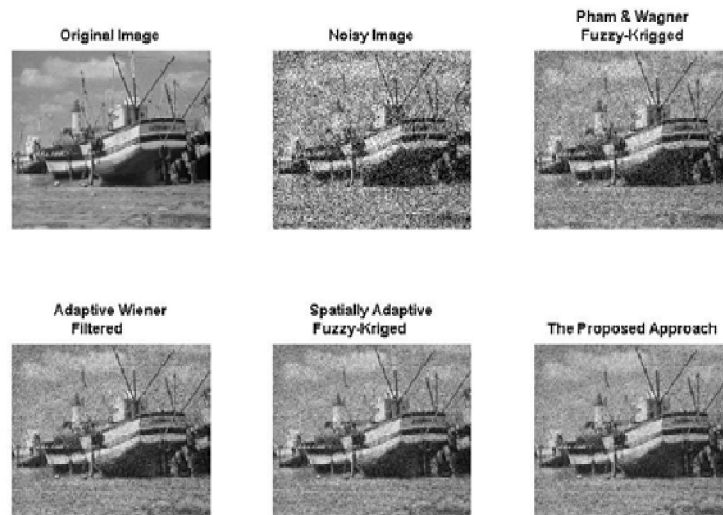


Figure 7. Original, noisy and estimated images obtained through PWFK, AWF, SAFK and proposed method

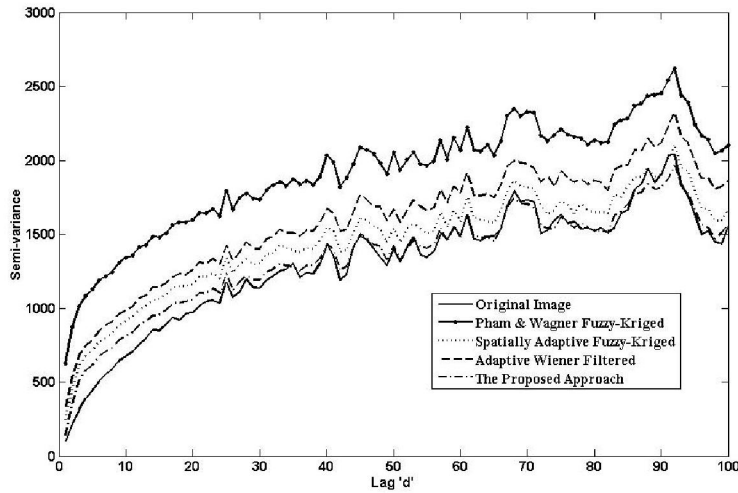


Figure 8. Comparison of the variograms of the original, degraded and processed Boat image
 Table 3. Comparison of de-noising methods for Boat image degraded with Gaussian white noise of different variances.

Noise Variance	Denoising Methods	Qualitative Measures			
		MSE	PSNR (db)	SSIM	VMSE
0.15	Noisy Image	6241.42	10.18	0.07	30278452.28
	PWFK	2087.54	14.93	0.14	2345782.40
	AWF	1161.52	17.48	0.22	294387.84
	SAFK	1124.02	17.62	0.22	254489.21
	The Proposed Approach	945.70	18.37	0.25	106559.78
0.14	Noisy Image	5990.28	10.36	0.07	27825746.76
	PWFK	1995.70	15.13	0.14	2012091.24
	AWF	1120.26	17.60	0.22	257448.74
	SAFK	1081.30	17.79	0.23	217489.04
	The Proposed Approach	903.28	18.54	0.26	82650.30
0.12	Noisy Image	5453.87	10.76	0.08	23363307.80
	PWFK	1785.23	15.61	0.15	1657722.31
	AWF	1027.38	17.97	0.24	240951.37
	SAFK	1004.80	18.11	0.25	183089.34
	The Proposed Approach	813.44	18.99	0.28	74764.22
0.1	Noisy Image	4829.47	11.29	0.09	18568778.65
	PWFK	1551.88	16.22	0.17	1229102.03
	AWF	921.16	18.43	0.26	233580.38
	SAFK	968.12	18.27	0.26	140906.53
	The Proposed Approach	717.38	19.53	0.30	61488.37
0.08	Noisy Image	4113.53	11.99	0.10	13719673.94
	PWFK	1305.34	16.97	0.19	834141.63
	AWF	796.36	19.02	0.29	219276.47
	SAFK	788.92	19.16	0.30	91159.31
	The Proposed Approach	609.64	20.18	0.33	44344.71
0.06	Noisy Image	3300.21	12.95	0.12	8998900.84
	PWFK	1035.00	17.98	0.23	508066.94
	AWF	650.50	19.91	0.32	169069.66
	SAFK	615.90	20.24	0.33	39738.01
	The Proposed Approach	493.35	21.12	0.37	29604.62
0.05	Noisy Image	2835.77	13.60	0.14	6754789.98
	PWFK	890.39	18.64	0.25	369484.11
	AWF	566.19	20.55	0.35	149426.04
	SAFK	521.50	20.94	0.35	26531.20
	The Proposed Approach	431.36	21.73	0.40	21467.21
0.03	Noisy Image	1808.72	15.56	0.19	2852017.75
	PWFK	585.86	20.45	0.32	131200.88
	AWF	371.95	22.33	0.44	77494.84
	SAFK	324.14	22.90	0.45	7801.69
	The Proposed Approach	294.27	23.34	0.47	7106.27
0.01	Noisy Image	632.77	20.12	0.34	369750.96
	PWFK	249.77	24.16	0.49	5559.37
	AWF	143.52	26.34	0.64	6764.69
	SAFK	141.56	26.36	0.64	6391.21
	The Proposed Approach	140.55	26.41	0.64	5905.73

The experimental variograms of the original, noisy, and restored images through AWF, PWFK, SAFK and proposed approach are plotted in Fig. 8. The image is corrupted with Gaussian noise of variance 0.08. From Fig. 8, it is clear that variograms of both the original as well as noisy image retain the structural information about the image and differ only in the semivariance at different lags depending upon the strength of the noise variance. Further, in comparison to the variograms produced by other methods, our approach produces a variogram that overlaps with the variogram of the original image. This is also clear from Table 3, where the VMSE is minimum compared to the other image restoration techniques.

4.3. Scenario 2

In the second case, we consider 450 different images as the test data. These images have been corrupted with white Gaussian noise of variance 0.05. Performance analysis of the above-mentioned methods is carried out in terms of average values of MSE, PSNR, SSIM, VMSE and VPSNR across 450 test images as shown in Table 4. The graphical representation of various performance measures is shown in Fig. 9. It can be observed that the performance of our proposed method is better as compared to PWFK, SAFK and AWF in terms of all of the image quality measures.

Table 4. Comparison of different methods across 450 test images.

Average Quality Measures	PWFK	AWF	SAFK	Neuro-Fuzzy Filter
MSE	910.07	592.18	543.28	475.97
PSNR	18.554	20.289	20.77	21.295
SSIM	0.2900	0.4024	0.40	0.4352
VMSE	235310	135470	132054	120410
VPSNR	0.00095	0.00211	0.00276	0.00333

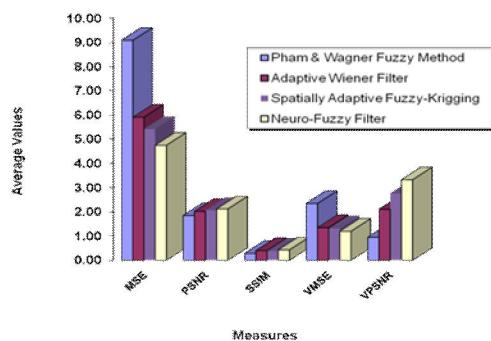


Figure 9. Comparison of different methods across test data of 450 images. Average values of various qualitative measures (note: the different image quality parameters are rescaled for elaboration purpose)

5. Conclusion

An effective hybrid image denoising method based on the concept of punctual kriging is analyzed. Fuzzy IF THEN rules based on region homogeneity and deviations, are used to intelligently decide the importance of a pixel in view of edge preservation. The method further solves the kriging matrix inversion and negative filter weights problems due to the learning capabilities of the neural net. The overall kriging procedure is coupled with a fuzzy smoothing filter. Due to the use of Fuzzy Decider, neural net is employed to estimate pixels along region boundaries and isolated discontinuities. However, for pixels inside the regions, away from the region boundaries, fuzzy smoothing is used. The results show a marked improvement in the performance of image restoration scheme as compared to the existing fuzzy kriging and adaptive Wiener filter approaches. In future work, we intend to increase the number of fuzzy rules for the better exploitation of the intensity variation on the edges, lines and object boundaries in the image.

Acknowledgements:

This research was supported by the MKE (The Ministry of Knowledge Economy), Korea, under the ITRC (Information Technology Research Center) support program supervised by the NIPA (National IT Industry Promotion Agency)" (NIPA-2012-H0301-12-3005) and BK21, South Korea under Postdoc fellowship.

Corresponding Author:

Dr. Asifullah Khan

Dept. of Computer Information & Science, PIEAS, P.O. Nilore, Islamabad, Pakistan

E-mail: asif@pieas.edu.pk

References

1. S. Voloshynovskiy, O. Koval, T. Pun, Image denoising based on the edge-process model, *Signal Process.* 85 (10) (2005) 1950-1969.
2. D. G. Krige, A Statistical Approach to Some Mine Valuation and Allied Problems on the Witwatersrand, Master Thesis, University of Witwatersrand, South Africa, 1951.
3. H. Wackernagel, *Multivariate Geostatistics: An Introduction with Applications*, Springer, 2003.
4. Y. S. Choi, R. Krishnapuram, A robust approach to image enhancement based on fuzzy logic, *IEEE Trans. Image Process.* 6 (6) (1997) 808-825.
5. M. Doroodchi, A. M. Reza, Implementation of fuzzy cluster filter for nonlinear signal and image processing, *Proc. IEEE Image Process. III* (1996) 2117-2122.
6. F. Farbiz, M. B. Menhaj, A fuzzy logic control based approach for image filtering, *Proc. Fuzzy Techniques in Image Process. LII* (2000) 194-221.
7. L. R. Liang, C. G. Looney, Competitive fuzzy edge detection, *Applied Soft Computing* 3 (2003) 123-137.

8. L. Khriji, M. Gabbouj, Rational-based adaptive fuzzy filters, *Int. J. Computational Cognition* 2 (1) (2004) 113–132.
9. W. Chua, L. Yang, Cellular networks: theory, *IEEE Trans. Circuits and Syst.* 35 (10) (1988) 1257–1272.
10. W. Chua, L. Yang, Cellular networks: applications, *IEEE Trans. Circuits and Syst.* 35 (10) (1988) 1273–1290.
11. M. Zamparelli, Genetically trained cellular neural networks, *Neural Networks* 10 (6) (1997) 1143–1151.
12. H. Hanek, N. Ansari, Speeding up the generalized adaptive neural filters, *IEEE Trans. Image Process.* 5 (5) (1996) 705–712.
13. Z. Z. Zhang, N. Ansari, Structure and properties of generalized adaptive neural filters for signal enhancement, *IEEE Trans. Neural Networks* 7 (4) (1996) 857–868.
14. N. Ansari, Z. Z. Zhang, Generalized adaptive neural filters, *IEE Electron Lett.* 29 (4) (1993) 342–343.
15. W. Qian, M. Kallergi, L.P. Clarke, Order statistic-neural network hybrid filters for gamma-camera-bremsstrahlung image restoration, *IEEE Trans. Medical Imaging* 12 (1) (1993) 58–64.
16. N. Suetake, E. Uchino, An RBFN–Wiener hybrid filter using higher order signal statistics, *Applied Soft Computing* 7 (2007) 915–922.
17. K. Sivakumar, U. B. Desai, Image restoration using a multilayer perceptron with a multilevel sigmoidal function, *Proc. IEEE Circuits and Syst.* (1992).
18. M. R. Widyanto, H. Nobuhara, K. Kawamoto, K. Hirota, B. Kusumoputro, Improving recognition and generalization capability of back-propagation NN using a self-organized network inspired by immune algorithm (SONIA), *Applied Soft Computing* 6 (2005) 72–84.
19. A. S. Palmer, M. Razaz, D. P. Mandic, Spatially adaptive image restoration by neural network filtering, *SBRN Symposium on Neural Networks* (2002) 184.
20. T. D. Pham, M. Wagner, Image enhancement by kriging and fuzzy sets, *Int. J. Pattern Recognition and Artificial Intelligence* 14 (8) (2000) 1025–1038.
21. T. D. Pham, M. Wagner, Filtering noisy images using kriging, *Int. Symp. Signal Process. & Applications* (1999).
22. A. M. Mirza, B. Munir, Combining fuzzy logic and kriging for image enhancement, *Proc. Fuzzy Days* (2004).
23. Asmatullah, Image Restoration using Machine Learning, Ph.D. Thesis, Faculty of Computer Science & Engineering, GIK Institute, Pakistan, 2007.
24. A. M. Mirza, Asmatullah, B. Munir, Spatially adaptive image restoration using fuzzy punctual kriging, *J. Computer Science and Technology* 22 (4) (2007) 580–589.
25. N. El-Sheimy, C. Valeo, A. Habib, *Digital Terrain Modeling: Acquisition, Manipulation and Applications*, Artech House Publishers, 2005.
26. D. Driankov, H. Hellendorn, M. Reinfrank, *An Introduction to Fuzzy Control*, Springer-Verlag, NY, 1993.
27. M. Sugeno, *Industrial Applications of Fuzzy Control*, Elsevier Science Publisher Co., 1985.
28. M. Nachtgeal, *Fuzzy Techniques in Image Processing*, Springer-Verlag LII (2000) 194–221.
29. P. Liu, H. Li, Fuzzy techniques in image restoration research – a survey, *Int. J. Computational Cognition* 2 (2) (2004) 131–149.
30. L. Rudasi, S. A. Zahorian, Pattern recognition using neural networks with a binary partitioning approach, *Proc. IEEE Southeastcon II* (1991) 726–730.
31. M.S. El Sherif, M.S. Abdel Samee, Pattern recognition using neural networks that learn from fuzzy rules, *Proc. Midwest Symposium on Circuits and Syst. I* (1994) 599–602.
32. H. Takahashi, N. Pecharanin, Y. Akima, M. Sone, The reliability of neural networks on pattern recognition, *Proc. IEEE Computational Intelligence Neural Networks V* (1994) 3067–3070.
33. A. Khan, A. Majid, T. S. Choi, Predicting protein subcellular location: exploiting amino acid based sequence of feature spaces and fusion of diverse classifiers, *Amino Acids* 38(1) (2010) 347–350.
34. A. Khan, S. F. Tahir, A. Majid, T. S. Choi, Machine learning based adaptive watermark decoding in view of an anticipated attack, *Pattern Recognition* 41 (2008) 2594–2610.
35. D. Greenhil, E. R. Davies, Relative effectiveness of neural networks for image noise suppression, *Proc. Pattern Recognition in Practice IV* (1994) 367–378.
36. T. M. Jochem, D. A. Pomerleau, C. E. Thorpe, Vision-based neural network road and intersection detection and traversal, *Proc. IEEE/RSJ Intelligent Robots and Syst. III* (1995) 344–349.
37. D. A. Pomerleau, *Neural Network Perception for Mobile Robot Guidance*, Ph.D. Thesis, Carnegie Mellon University, 1992.
38. A. Chaudhry, A. Khan, A. M. Mirza, A. Ali, A hybrid image restoration approach: using fuzzy punctual kriging and genetic programming, *Int. J. Imaging Syst. and Technology* 17 (4) (2007) 224–231.
39. H. Tizhoosh, Fuzzy image enhancement: an overview, *Fuzzy Techniques in Image Processing*, Springer-Verlag LII (2000) 137–171.
40. Asmatullah, A.M. Mirza, A. Khan, Blind image restoration using multilayer backpropagator, *Proc. IEEE INMIC* (2003) 55–58.